Pergamon

Computers & Structures Vol. 65, No. 2, pp. 255–259, 1997

Printed in Great Britain
0045-7949/97 $17.00 + 0.00

PII: S0045-7949(96)00269-6

OPTIMUM DESIGN OF HIGH-SPEED FLEXIBLE ROBOTIC ARMS WITH DYNAMIC BEHAVIOR CONSTRAINTS

S. Oral and **S. Kemal Ider**
Department of Mechanical Engineering, METU, Ankara 06531, Turkey

(*Received* 31 *May* 1995)

Abstract—A methodology is presented for the optimum design of robotic arms under time-dependent stress and displacement constraints by using mathematical programming. Finite elements are used in the modeling of the flexible links. The design variables are the cross-sectional dimensions of the elements. The time dependence of the constraints is removed through the use of equivalent constraints based on the most critical constraints. It is shown that this approach yields a better design than using equivalent constraints obtained by the Kresselmeier–Steinhauser function. An optimizer based on sequential quadratic programming is used and the design sensitivities are evaluated by overall finite differences. The dynamical equations contain the nonlinear interactions between the rigid and elastic degrees-of-freedom. To illustrate the procedure, a planar robotic arm is optimized for a particular deployment motion by using different equivalent constraints. © 1997 Elsevier Science Ltd.

1. INTRODUCTION

The increasing demand for high-speed robots has made it necessary to use components that must be designed for minimum weight. The traditional design of robotic arms based on multiple postures in static regime is not suitable for high-speed systems where the stresses and deflections are governed by the dynamic effects. To prevent failure, intricate interactions between the rigid and elastic motions must be taken into account in the design.

The design of structural systems under transient loading has been studied by using different equivalent constraints based on critical point selection [1], time integral of violated constraints [2], and Kreisselmeier–Steinhauser function [3, 4]. In critical point selection, it is assumed that the location of the critical points are assumed to be fixed in time, however this assumption is not appropriate for high-speed multibody systems. The second approach has the disadvantage that the equivalent constraint is zero in the feasible domain and hence there is no indication when the constraint is almost critical. The use of Kreisselmeier–Steinhauser function results in an equivalent constraint which is nonzero in the feasible domain, however it defines a conservative envelope and yields oversafe designs.

In the design of robotic arms, the conventional approach is to consider multiple static postures [5–7] rather than considering the time-dependency of the constraints. This approach is not appropriate for high-speed systems, since a few postures cannot represent the overall system motion, and furthermore the displacements and stresses computed are inaccurate due to omitting the coupling between rigid and elastic motions. In fact, this coupling is the essence of a flexible multibody analysis [8–10].

In this study, a methodology for the design of high-speed robotic arms is developed considering the coupled rigid–elastic motion of the system and the time-dependency of the constraints. The most critical constraints are used as the equivalent constraints. The time points of the most critical constraints may vary as the design variables change. The sensitivity of the response is evaluated by overall finite differences and the optimization is carried out by sequential quadratic programming [11]. To illustrate the procedure, a two-link planar robotic arm is optimized for strength and rigidity. The results are compared with those obtained by using the Kreisselmeier–Steinhauser function.

2. DESIGN PROBLEM

In this section, the optimum design of a robotic arm is formulated as a nonlinear mathematical programming problem for strength and rigidity. The arm consists of N number of flexible links each of which are discretized by E_k number of beam finite elements. The objective is to minimize the weight of the arm. The contraints related to strength are the element stresses and the constraints for rigidity are the deviations of the selected points from the path of the rigid model. The design variables are the cross-sectional properties of the link elements.

Mathematically, this is written as

$$\text{minimize the objective function } f = \sum_{k=1}^{N}\sum_{i=1}^{E_k} \rho^{ki} V^{ki}$$

$$\text{subject to constraints } g_j(\mathbf{x}, t) > 0 \quad j = 1, \dots, N_c, \tag{1}$$

where ρ^{ki} and V^{ki} are the mass density and volume of the ith element of kth body, respectively, $\mathbf{x}$ is the vector of N_v number of design variables and N_c is the total number of time-dependent constraints. In evaluating the displacements and stresses, the following recursive formulation based on Ref. [10] is employed to model the coupled rigid–elastic motion of the arm.

Let the deformation of a link B_k be defined relative to a link reference frame ξ^k which follows the global motion of B_k in a manner consistent with the boundary conditions. The number of elastic degrees-of-freedom of each link is reduced by modal reduction.

The generalized coordinates of the system are the joint variables θ_i and modal variables η_i. The velocity of a particle P, v^{ki}, can be written as

$$v^{ki} = \gamma^{ki}\dot{\theta} + \beta^{ki}\dot{\eta}, \tag{2}$$

where γ^{ki} and β^{ki} are the corresponding influence coefficient matrices.

Kane *et al.*'s equations [12] are used to determine the equations of motion as

$$\mathbf{M}\dot{\mathbf{y}} = \mathbf{Q} + \mathbf{F}^s + \mathbf{F}, \tag{3}$$

where $\mathbf{y} = [\dot{\theta}^T, \dot{\eta}^T]^T$ is the vector of generalized speeds, $\mathbf{F}$ is the vector of generalized applied forces, and $\mathbf{M}$, $\mathbf{Q}$ and $\mathbf{F}^s$ are the generalized masses, Coriolis and centrifugal forces and elastic forces, respectively, as shown below:

$$\mathbf{M} = \begin{bmatrix} \mathbf{M}^{rr} & \mathbf{M}^{rf} \\ \text{sym.} & \mathbf{M}^{ff} \end{bmatrix} = \sum_{k=1}^{N}\sum_{i=1}^{E_k} \rho^{ki} \int_{V^{ki}} \begin{bmatrix} \gamma^{ki^T}\gamma^{ki} & \gamma^{ki^T}\beta^{ki} \\ \text{sym.} & \beta^{ki^T}\beta^{ki} \end{bmatrix} \mathrm{d}V \tag{4}$$

$$\mathbf{Q} = \begin{bmatrix} \mathbf{Q}^r \\ \mathbf{Q}^f \end{bmatrix} = -\sum_{k=1}^{N}\sum_{i=1}^{E_k} \rho^{ki} \int_{V^{ki}} \begin{bmatrix} \gamma^{ki^T} \\ \beta^{ki^T} \end{bmatrix} (\dot{\gamma}^{ki}\dot{\theta} + \dot{\beta}^{ki}\dot{\eta})\mathrm{d}V \tag{5}$$

$$\mathbf{F}^s = -\begin{bmatrix} 0 \\ \mathbf{K}\eta \end{bmatrix} \tag{6}$$

where the superscripts r and f refer to rigid body and elastic degrees-of-freedom, respectively. $\mathbf{K}$ is a block diagonal matrix whose diagonal submatrices are the reduced stiffness matrices of B_k in terms of modal variables. To evaluate the submatrices in eqns (4, 5), γ^{ki} and β^{ki} are expressed in the following form as:

$$\gamma^{ki}_{pq} = \bar{\gamma}^{k}_{pq} + \tilde{\gamma}^{ki}_{pqrs}\phi^{ki}_{rs} \quad p, r = 1, 2, 3 \quad q = 1, \dots, n_r \quad s = 1, \dots, 12 \tag{7a}$$

$$\beta^{ki}_{pq} = \bar{\beta}^{k}_{pq} + \tilde{\beta}^{ki}_{pqrs}\phi^{ki}_{rs} \quad p, r = 1, 2, 3 \quad q = 1, \dots, m \quad s = 1, \dots, 12, \tag{7b}$$

where ϕ^{ki} is the element shape function, n_r is the number of joint variables and m is the number of modal variables. Note that in the equations, a repeated subscript index in a term implies summation. Superscripts are generally part of the labeling and do not imply summation unless otherwise specified. The mass submatrices can be written as

$$\mathbf{M}^{rr}_{qt} = \sum_{k=1}^{N}\sum_{i=1}^{E_k} [m^{ki}\bar{\gamma}^{k}_{pq}\bar{\gamma}^{k}_{pt} + (\bar{\gamma}^{k}_{pq}\tilde{\gamma}^{ki}_{ptzs} + \bar{\gamma}^{k}_{pt}\tilde{\gamma}^{ki}_{pqzs})P^{ki}_{zs} + \tilde{\gamma}^{ki}_{pqzs}\tilde{\gamma}^{ki}_{ptuv}R^{ki}_{zusv}] \tag{8a}$$

$$\mathbf{M}^{ff}_{qt} = \sum_{k=1}^{N}\sum_{i=1}^{E_k} [m^{ki}\bar{\beta}^{k}_{pq}\bar{\beta}^{k}_{pt} + (\bar{\beta}^{k}_{pq}\tilde{\beta}^{ki}_{ptzs} + \bar{\beta}^{k}_{pt}\tilde{\beta}^{ki}_{pqzs})P^{ki}_{zs} + \tilde{\beta}^{ki}_{pqzs}\tilde{\beta}^{ki}_{ptuv}R^{ki}_{zusv}] \tag{8b}$$

$$\mathbf{M}^{rf}_{qt} = \sum_{k=1}^{N}\sum_{i=1}^{E_k} [m^{ki}\bar{\gamma}^{k}_{pq}\bar{\beta}^{k}_{pt} + (\bar{\gamma}^{k}_{pq}\tilde{\beta}^{ki}_{ptzs} + \bar{\beta}^{k}_{pt}\tilde{\gamma}^{ki}_{pqzs})P^{ki}_{zs} + \tilde{\gamma}^{ki}_{pqzs}\tilde{\beta}^{ki}_{ptuv}R^{ki}_{zusv}] \tag{8c}$$

where

$$P^{ki}_{ut} = \int_{V^{ki}} \rho^{ki}\phi^{ki}_{ut}\mathrm{d}V \text{ and } R^{ki}_{zusv} = \int_{V^{ki}} \rho^{ki}\phi^{ki}_{zs}\phi^{ki}_{uv}\mathrm{d}V;$$

$$z, u = 1, 2, 3; \quad s, v = 1, \dots, 12$$

are the time-invariant matrices, and m^{ki} is the mass of ith finite element of the kth body. By defining $a^k_m = \dot{\bar{\gamma}}^k_{mq}\dot{\theta}_q + \dot{\bar{\beta}}^k_{mp}\dot{\eta}_p$ and $b^{ki}_{mru} = \dot{\tilde{\gamma}}^{ki}_{mqru}\dot{\theta}_q + \dot{\tilde{\beta}}^{ki}_{mpru}\dot{\eta}_p$, the Coriolis and centrifugal forces can be computed as

$$\mathbf{Q}^r_q = \sum_{k=1}^{N}\sum_{i=1}^{E_k} [m^{ki}\bar{\gamma}^{k}_{pq}a^k_p + (\bar{\gamma}^{k}_{pq}b^{ki}_{pzs} + a^k_p\tilde{\gamma}^{ki}_{pqzs})P^{ki}_{zs} + \tilde{\gamma}^{ki}_{pqzs}b^{ki}_{puv}R^{ki}_{zusv}] \tag{9a}$$

$$\mathbf{Q}^f_q = \sum_{k=1}^{N}\sum_{i=1}^{E_k} [m^{ki}\bar{\beta}^{k}_{pq}a^k_p + (\bar{\beta}^{k}_{pq}b^{ki}_{pzs} + a^k_p\tilde{\beta}^{ki}_{pqzs})P^{ki}_{zs} + \tilde{\beta}^{ki}_{pqzs}b^{ki}_{puv}R^{ki}_{zusv}]. \tag{9b}$$

The equations of motion are integrated by using a variable step, variable order predictor–corrector algorithm to obtain the time history of the generalized coordinates θ_i and η_i. Then nodal displacements with respect to the body reference frames are obtained by the modal transformation of η_i. The element stresses are computed by the stress–displacement relations. The displacements of the points of interest in the global reference frame are found by using θ_i and the nodal displacements in the body frames. The deviation of a point is defined as the difference between the global displacements of that point in the flexible and rigid models.

It should be noted that, in the equations of motion, the only terms that are functions of design variables are the stiffness matrix, the element masses and the arrays P^{ki} and R^{ki} in the mass matrix and load vector. Hence in the analytical sensitivity analysis, these are the terms that should be differentiated with respect to the design variables. However, analytical evaluation of the sensitivities is a difficult task in this class of problems. A semi-analytical or overall finite difference approach is much better suited.

3. CONSTRAINT REDUCTION

The dynamic response of the arm is calculated at N_t number of discrete points in the time domain. Hence, the number of constraints to be satisfied becomes $N_c \times N_t$, and such a large number of constraints is not practical in an optimization process. An effective approach to keep the number of constraints as N_c and to ensure satisfaction of constraints for all values of t is to define equivalent time-independent constraints by using Kreisselmeier–Steinhauser function [3] as

$$\bar{g}_j(\mathbf{x}) = -\frac{1}{c}\ln\sum_{n=1}^{N_t}\exp(-cg_{jn}) \qquad (10)$$

where $g_{jn}(\mathbf{x}) = g_j(\mathbf{x}, t_n)$ and c is a user-selected positive number which determines the relation between $\bar{g}_j$ and the most critical g_{jn}, i.e. $\min(g_{jn})$. It can be shown that the Kreisselmeier–Steinhauser function defines a conservative envelope [4] such that $\bar{g}_j$ is always more critical than $\min(g_{jn})$, and the larger the value of c, the closer $\bar{g}_j$ follows $\min(g_{jn})$. This suggests using the most critical constraint as the equivalent constraint as

$$\bar{g}_j(\mathbf{x}) = \min[g_{jn}(\mathbf{x})]. \qquad (11)$$

In this approach, the equivalent constraint $\bar{g}_j$ defines a piecewise-smooth function with finite discontinuous gradients as it makes transitions from g_{jp} to g_{jq}. In this envelope, although the right- and left-hand derivatives are different at the transition points, they are of the same sign and the gradients are blended at the transition points by the numerical differentiation. In the limit as the time step approaches zero, the equivalent constraint becomes smooth.

The nonlinear, constrained optimization problem defined above is solved by using the optimizer NLPQL [11] which is based on sequential quadratic programming. This optimizer requires first-order information $\mathrm{d}f/\mathrm{d}x_m$ and $\mathrm{d}\bar{g}_j/\mathrm{d}x_m$, $m = 1, \ldots, N_v$, which are computed by overall finite differences in the present work.

4. NUMERICAL EXAMPLE

A two-link planar robot is shown in Fig. 1. A single task is considered in which the end-effector E is required to deploy from an initial position ($\theta_1 = 120°$, $\theta_2 = -150°$) to a final position ($\theta_1 = 60°$, $\theta_2 = -30°$) along a straight line. The prescribed motion of E is given as

$$\Delta X_E = \Delta Y_E = \frac{0.5}{T}\left(t - \frac{T}{2\pi}\sin\frac{2\pi t}{T}\right).$$

The period of the deployment motion, T, is taken to be 0.5 s.

Each link is of length 0.6 m and is modeled by two equal length tubular Euler beam finite elements. The outer diameters, D_{ki}, $k = 1, 2$; $i = 1, 2$ of the elements are taken as the design variables. The wall thickness of each element is set to be $0.1D_{ki}$. The material properties are $E = 72$ GPa and $\rho = 2700$ kg m^{-3}. The problem size is reduced by using modal variables. The first two bending modes and the first axial mode with fixed–free boundary conditions are considered. The

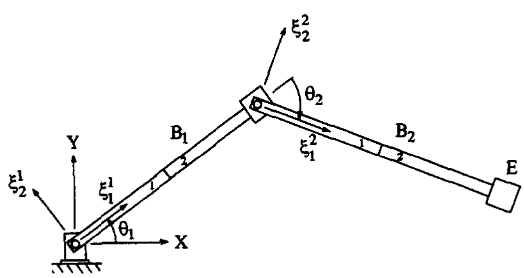

Fig. 1. A planar robotic manipulator.

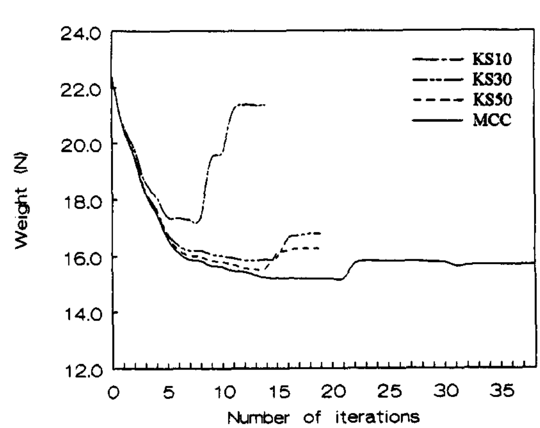

Fig. 2. Design histories.

Table 1. Optimum solutions for the planar robotic manipulator

	Weight (N)	D_{11} (mm)	D_{12} (mm)	D_{21} (mm)	D_{22} (mm)	Number of iterations
KS-10	21.374	62.635	50.982	45.107	30.927	14
KS-30	16.800	55.995	45.409	39.266	27.172	19
KS-50	16.286	55.210	44.742	38.524	26.736	19
MCC	15.719	54.266	44.150	37.552	26.315	38

actuator of link-2 is located at joint-B has a mass of 2 kg and the combined mass of the end-effector and payload is 1 kg.

The design problem is solved under the following constraints:

$$-75\text{ MPa} \leqslant \sigma_i \leqslant 75\text{ MPa} \quad i = 1, \ldots, n_s$$

$$\delta \leqslant 0.001\text{ m},$$

where the stress constraints are evaluated at n_s number of points which are the top and bottom points at each node. δ is the deviation (magnitude of the resultant of deviations in x and y directions) of the end-effector E from the rigid motion. The initial design is 50 mm for all design variables, D_{ki}.

In this example, the equivalent constraints are formed by employing the most critical constraints and the results are compared by using the Kreisselmeier–Steinhauser function. In the latter, different values of c have been tried. It has been observed that the lower values of c resulted in highly conservative designs, as expected. A value of $c = 50$ yielded a satisfactory design. It should be noted that the compiler limits may be exceeded for large values of c due to the exponential function if the lower bounds on design variables are set too small. On the other hand, the most critical constraint approach resulted in the lightest design satisfying the deviation constraint exactly. The minimum weights, optimum diameters and number of iterations are tabulated in Table 1. The design histories are shown in Fig. 2. The labels KS-c denote the results obtained by the Kreisselmeier–Steinhauser function, whereas MCC denotes the use of most critical constraint approach. It is seen that the stresses are far below the allowable

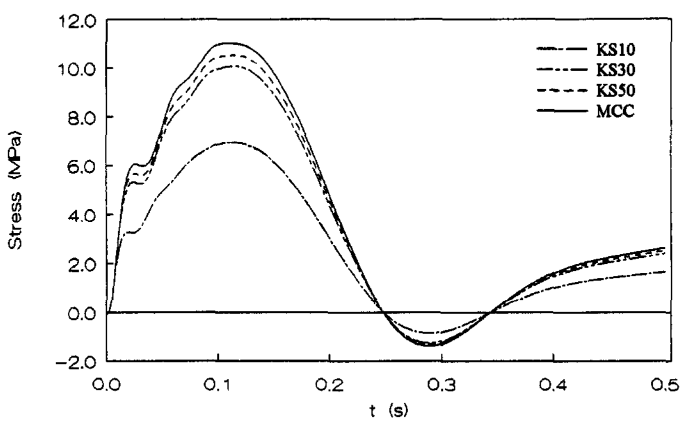

Fig. 3. The stresses at the middle of link-2 at the top in the optimum designs.

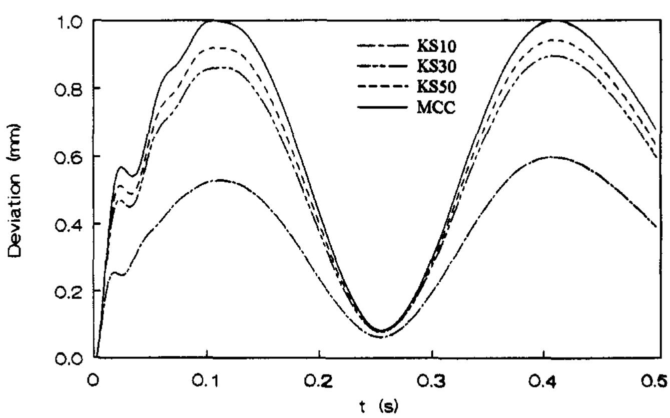

Fig. 4. The end-effector deviation in the optimum designs.

values, hence the stress constraints are inactive. The stresses at the middle of link-2 at the top, where the maximum stresses occur, are plotted in Fig. 3. The end-effector deviation δ for the optimum solution is shown in Fig. 4.

5. CONCLUSIONS

In this study, a methodology for the optimum design of high-speed robotic manipulators subject to dynamic response constraints has been presented. The coupled rigid–elastic motion of the manipulator has been considered. The large number of time-dependent constraints has been reduced by forming equivalent time-independent constraints based on the most critical constraints whose time points may vary as the design variables change. It has been shown that the piecewise-smooth nature of this equivalent constraint does not cause a deficiency in the optimization process. Sequential quadratic programming is used in the solution of the design problem with sensitivities calculated by overall finite differences. A high-speed planar robotic manipulator has been optimized for minimum weight under stress and deviation constraints. The use of equivalent constraints based on Kreisselmeier–Steinhauser function yielded conservative designs, while the most critical constraint approach resulted in the best design.

REFERENCES

1. W. H. Greene and R. T. Haftka, Computational aspects of sensitivity calculations in transient structural analysis. *Comput. Struct.* **32,** 433–443 (1989).
2. E. J. Haug and J. S. Arora, Design sensitivity analysis of elastic mechanical systems. *Comput. Meth. appl. Mech. Engng* **15,** 35–62 (1978).
3. G. Kreisselmeier and R. Steinhauser, Systematic control design by optimizing a vector performance index. In: *Proc. IFAC Symp. Computer Aided Design of Control Systems*, Zurich, pp. 113–117 (1979).
4. R. T. Haftka, Z. Gurdal and M. P. Kamat, *Elements of Structural Optimization*. Kluwer Academic, Dordreicht (1990).
5. D. A. Saravanos and J. S. Lamancusa, Optimum structural design of robotic manipulators with fiber reinforced composite materials. *Comput. Struct.* **36,** 119–132 (1990).
6. M. H. Korayem and A. Basu, Formulation and numerical solution of elastic robot dynamic motion with maximum load carrying capacities. *Robotica* **12,** 253–261 (1994).
7. J. H. Park and H. Asada, Concurrent design optimization of mechanical structure and control for high speed robots. *ASME J. Dyn. Systems, Mesmt Control* **116,** 344–356 (1994).
8. A. A. Shabana, *Dynamics of Multibody Systems*. Wiley, New York (1989).
9. S. S. Kim and E. J. Haug, A recursive formulation for flexible multibody dynamics, Part 1: open loop systems. *Comput. Meth. appl. Mech. Engng* **71,** 293–314 (1988).
10. S. K. Ider and F. M. L. Amirouche, Nonlinear modeling of flexible multibody systems dynamics subjected to variable constraints. *ASME J. appl. Mech.* **56,** 444–451 (1989).
11. K. Schittkowski, NLPQL-A Fortran subroutine solving constrained nonlinear programming problems. *Ann. Opns Res.* **5,** 485–500 (1985).
12. T. R. Kane, P. W. Likins and D. A. Levinson, *Spacecraft Dynamics*. McGraw-Hill, New York (1983).